Electronic Supplementary Information

Electron-Donating Strength Dependent Symmetry Breaking Charge Transfer Dynamics of Quadrupolar Molecules

Xinmiao Niu,[a,b,†] *Zhuoran Kuang,* [a,b,†] *Miquel Planells,*[c] *Yuanyuan Guo,* [a,b] *Neil Robertson,**[c] *Andong Xia**[a,b]

[a] Beijing National Laboratory for Molecular Sciences (BNLMS), Key laboratory of Photochemistry, Institute of Chemistry, Chinese Academy of Sciences, Beijing 100190, People's Republic of China

[b] University of Chinese Academy of Sciences, Beijing 100049, People's Republic of China

[c]EastChem – School of Chemistry, University of Edinburgh, Kings Buildings, Edinburgh EH9 3JJ, UK.

E-mail: andong@iccas.ac.cn ; neil.robertson@ed.ac.uk

Table of Contents

S1. Details of the transient absorption spectral and transient fluorescence spectral measurements.

Femtosecond transient absorption spectra.

Transient absorption measurements with a time resolution of ~90 fs were performed by using a homemade femtosecond broadband pump-probe setup.[1, 2] In brief, a pulse with 400 nm, 90 nJ produced by doubling a portion of the 800 nm pulse with a BBO (type I, 0.5 mm thickness) crystal from regenerative amplified femtosecond laser (50 fs, 1 kHz, Coherent Legend Elite U.S.A.) acts as the pump beam (spot size at the sample is ca. 130 μm). A white light super continuum (420-780 nm) generated by a water cell acts as probe beam with an optical delay up to >1 ns. For isotropic measurements, the included angle between the pump and probe beam polarization was set to the magic angle (54.7°).

Femtosecond time-resolved transient fluorescence

Femtosecond transient fluorescence spectra were conducted on a fluorescence up-conversion spectrophotometer.[3] The system was pumped by a regenerative amplified femtosecond Ti: sapphire laser (Legend Elite, Coherent) centered at 800 nm (1000 Hz, ~50 fs, ~1.0 mJ). The light beam was frequency-doubled in a BBO (type I) crystal and a dichroic mirror was used to separate the fundamental from the doubled beam (400 nm) sent for the fluorescence excitation. The remained fundamental light was time-delayed and used to gate the emission of the sample that flew in a 1-mm quartz cell. The collected fluorescence was focused onto a BBO crystal (type I, cut angle Theta = 35 degree) using reflective optics. The gating pulse was also focused onto the crystal overlapping with the fluorescence. The included angle between the excitation and gating beam polarization was set to the magic angle (54.7°). The up-converted signal was filtered and detected with a photomultiplier tube. The instrument response function of the system measured by gating the Raman signal from solvent was ~300 fs.

S2. Calculation of the emission dipole moment.

The steady-state emission dipole moment is calculated by equation S1 as follows,[4]

$$\mu_{em} = 1.7857 \times 10^{3} \left[\frac{k_r}{n^3 f(n) \tilde{\nu}_f^3} \right]^{1/2} \quad \text{(S1)}$$

where k_r is the radiative rate constant, n is the refractive index of solvent, $f(n)$ is an effective cavity factor, is represented by equation S2,

$$f(n) = \frac{9n^2}{(2n^2+1)^2} \quad \text{(S2)}$$

and $\tilde{\nu}_f^3$ is the cube of emission frequency,[5] defined by

$$\tilde{\nu}_f^3 = \frac{\int F(\nu)\nu^3 d\nu}{\int F(\nu)\, d\nu} \quad \text{(S3)}$$

, where ν is the wavenumber and $F(\nu)$ denotes the fluorescence spectrum after the correction of the instrument spectral response.

The obtained steady-state emission dipole moment is denoted as $\mu_{em}(S)$. Using this quantify, the time-dependent instantaneous emission dipole moment is obtained by equation S4,

$$\mu_{em}(t) = \mu_{em}(s) \cdot \sqrt{\int_{\nu_1}^{\nu_2} F_\tau(t) / \int_{\nu_1}^{\nu_2} F_\tau(> 200\, ps)} \quad \text{(S4)}$$

, where F_τ(t) is the corrected fluorescence intensity for population decay using equation S5,

$$F_\tau(t) = \frac{F(t)}{\exp(-t/\tau)} \quad \text{(S5)}$$

Since this dynamic process include solvation, structural relaxation, 200 ps is an adequate time to use F_τ(t>200 ps) as a normalization factor.

S3. Electronic-state transitions.

Table S1. Electronic transition properties of **Me-DATPA** and **MeO-DATPA** in gas phase at their optimized ground state geometries at the TD-DFT/CAM-B3LYP/6-31G(d) level.

	Me-DATPA	**MeO-DATPA**
	S_1	S_1
E (eV)	3.50 eV (354 nm)	3.51eV (353 nm)
oscillator strength	2.1646	2.2836
main orbital contribution	HOMO→LUMO 0.639 HOMO-2→LUMO 0.144	HOMO→LUMO 0.636 HOMO-2→LUMO 0.161

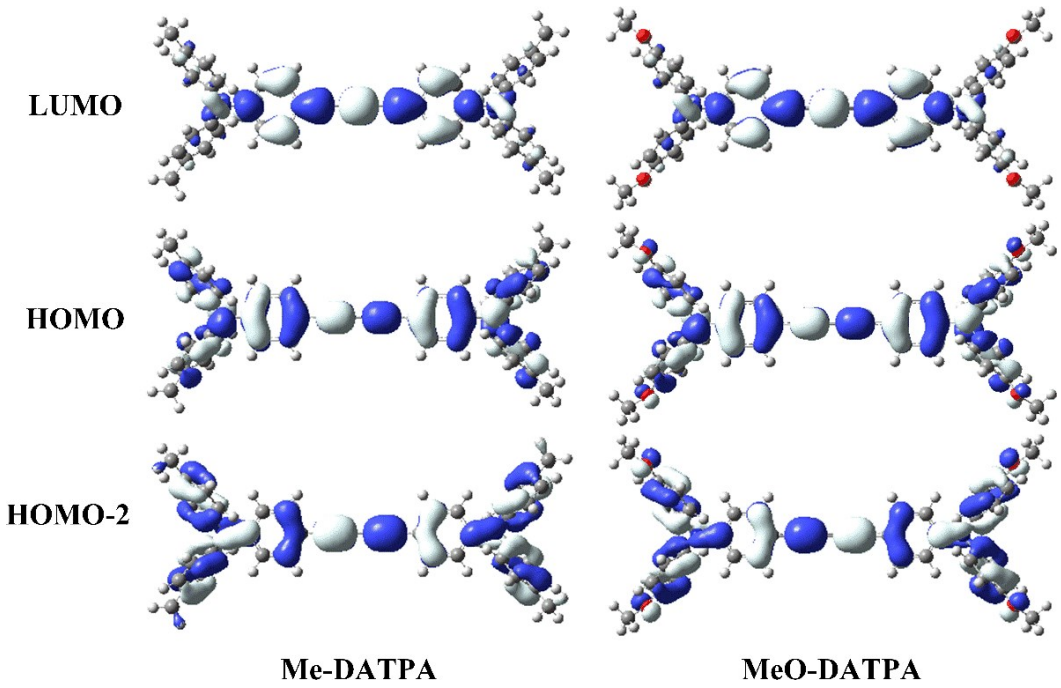

Figure S1. Electron density contours of molecular orbitals LUMO, HOMO, HOMO-2 at S_0 geometries of **Me-DATPA** and **MeO-DATPA** in the gas phase.

S4. Steady-state spectral data.

Table S2. Absorption, fluorescence and solvents parameters.

			Me-DATPA			MeO-DATPA			
solvent	Abbr.	Δf [a]	λ_{abs} (nm)	λ_{flu} (nm)	Stokes Shifts (cm^{-1})	Δf	λ_{abs} (nm)	λ_{flu} (nm)	Stokes Shifts (cm^{-1})
Cyclohexane	CHX	0	376	418	2672	0	379	428.4	3043
Di-n-butyl Ether	DBE	0.095	376	423.4	2977	0.095	378	438.6	3655
Diethyl ether	DEE	0.163	377	426	3051	0.163	379	445.8	3954
Butyl acetate	BA	0.17	377	432.2	3388	0.17	378	456	4525
Ethyl acetate	EA	0.2	378	435.6	3498	0.2	382	463.8	4617
Tetrahydrofuran	THF	0.21	379	438.6	3585	0.21	386	466	4448
Acetone	ACE	0.285	375	455.8	4727	0.285	377	502.6	6629

[a] The polarity indices are taken from Ref 6.[6]

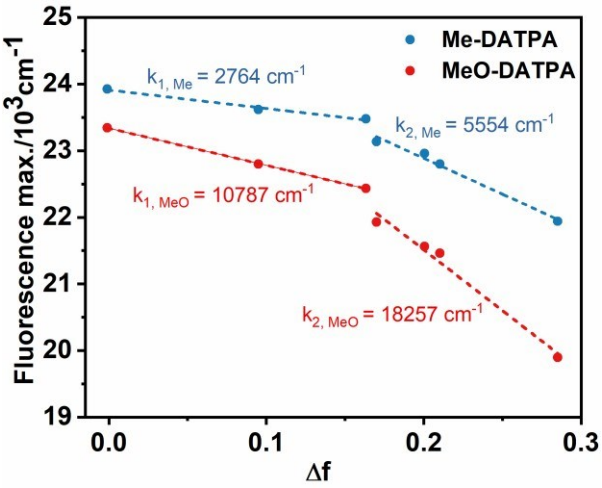

Figure S2. Fluorescence maximum of both molecules as a function of the solvent orientation polarizability and best linear fits.

Table S3. Slopes of the linear fit of the fluorescence maximum of **Me-DATPA** and **MeO-DATPA** against with solvent polarizability $\Delta f = \frac{(\varepsilon-1)}{(2\varepsilon+1)} - \frac{(n^2-1)}{(2n^2+1)}$. k_1 corresponds to the initial slope from the nonpolar to medium polar solvents, while k_2 represents the slope from medium polar to highly polar solvents. (Figure S1)

	k_1 (cm^{-1})	k_2 (cm^{-1})
Me-DATPA	2764	5554
MeO-DATPA	10787	18257

Table S4. Photophysical properties of **Me-DATPA** and **MeO-DATPA**.

	Me-DATPA				MeO-DATPA			
solvent	Φ_f	τ (ns)	k_r [b]($\times 10^8$ s^{-1})	k_{nr} [b]($\times 10^8$ s^{-1})	Φ_f	τ (ns)	k_r [b]($\times 10^8$ s^{-1})	k_{nr} [b]($\times 10^8$ s^{-1})
Cyclohexane	0.73	0.68	10.74	3.97	0.77	0.83	9.28	2.77
Di-n-butyl Ether	0.58	0.77	7.53	5.45	0.59	1.02	5.78	4.02
Diethyl ether	0.58	0.83	6.99	5.06	0.51	1.27	4.02	3.86
Butyl acetate	0.57	0.85	6.71	5.06	0.50	1.43	3.50	3.50
Ethyl acetate	0.49	0.89	5.51	5.73	0.42	1.66	2.53	3.49
Tetrahydrofuran	0.41	0.9	4.56	6.56	0.30	1.67	1.80	4.19
Acetone	0.32	1.27	2.52	5.35	0.21	2.16	0.97	3.66

[b] Rate constants of radiative k_r and nonradiative k_{nr} are calculated using equantions □□ = □/□ and □□ + □□□ = □/□.

S5. Fluorescence lifetime measurements.

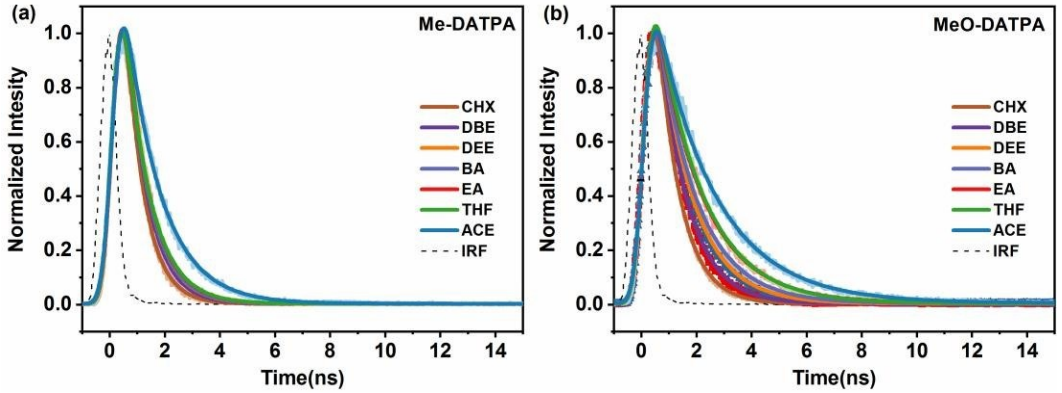

Figure S3. Fluorescence lifetimes of (a) dye **1** and (b) dye **2**. Fitting results are also included.

S6. Femtosecond transient absorption experiments.

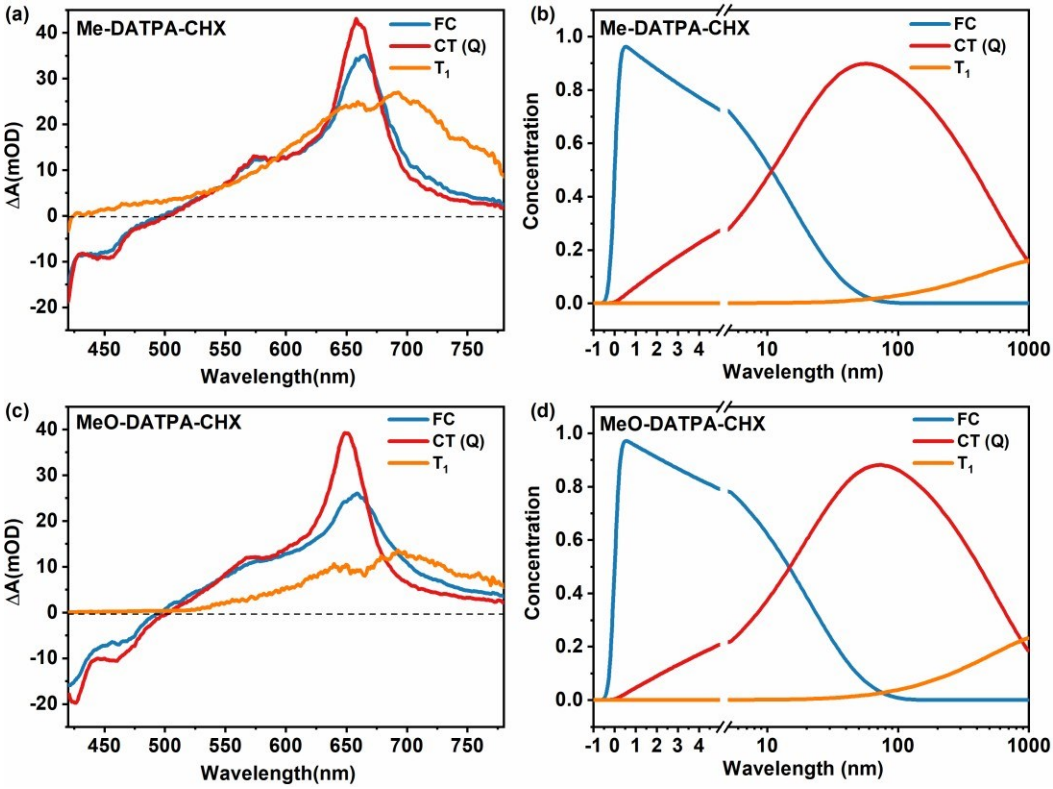

Figure S4. SADSs from target analysis and concentration evolution of transient species of **Me-DATPA** and **MeO-DATPA** in CHX.

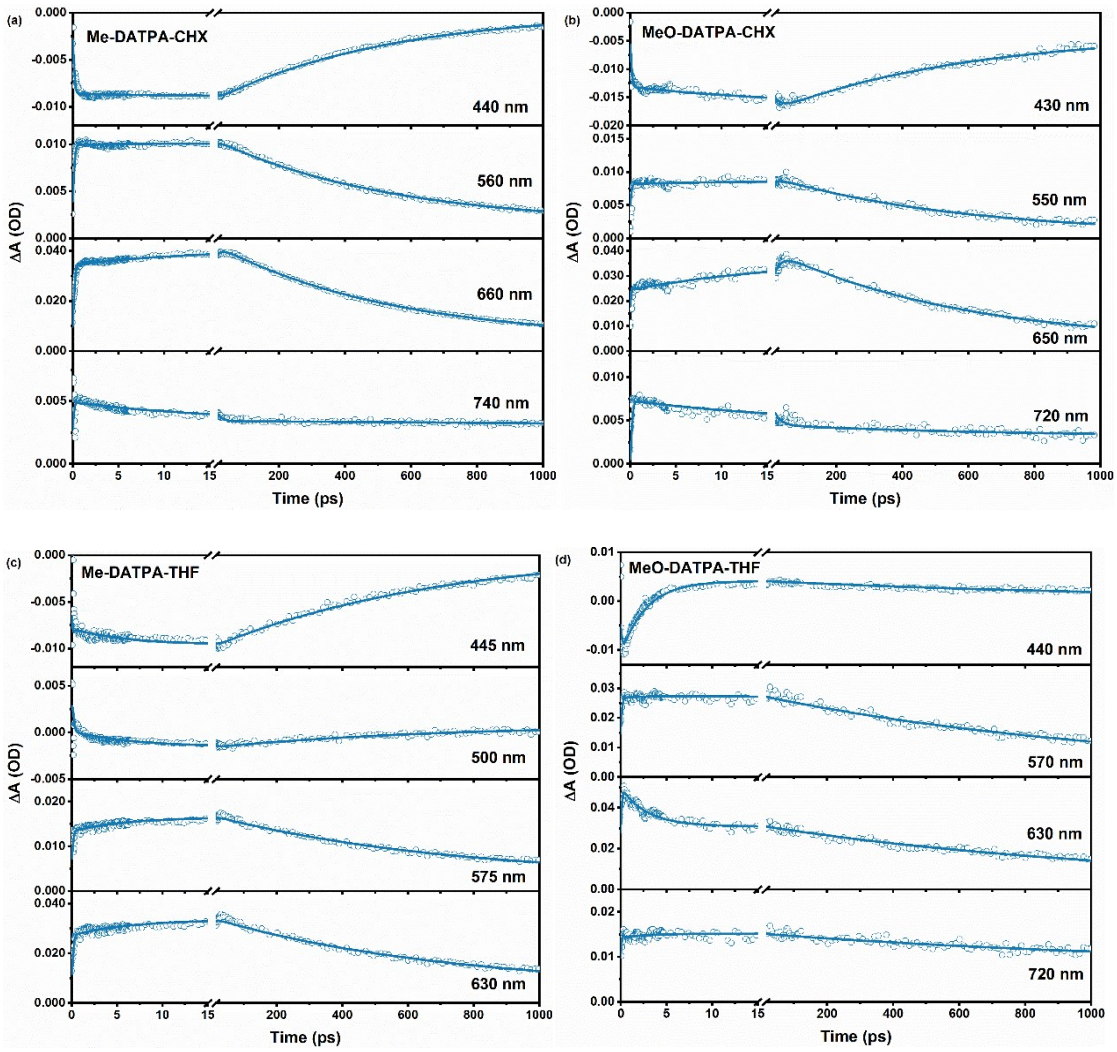

Figure S5. Kinetics of femtosecond transient absorption spectra of **Me-DATPA** and **MeO-DATPA** in CHX and THF at selected wavelengths are plotted (dot) together with global fitting curves (line) of all collected time traces. For **Me-DATPA** in CHX, 440, 560, 660 and 740 nm wavelengths are selected (a), and for **MeO-DATPA** in CHX, 430, 550, 650 and 720 nm wavelengths are selected (b). For **Me-DATPA** in THF, 445, 500, 575 and 630 nm wavelengths are selected (c), and for **MeO-DATPA** in THF, 440, 570, 630 and 720 nm wavelengths are selected (d).

S7. Nanosecond transient absorption experiments.

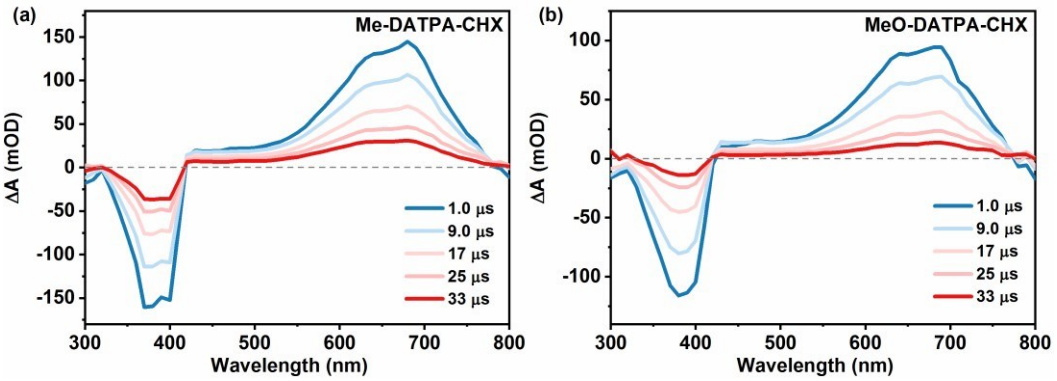

Figure S6. Nanosecond transient absorption spectra of **Me-DATPA** (a) and **MeO-DATPA** (b) in CHX.

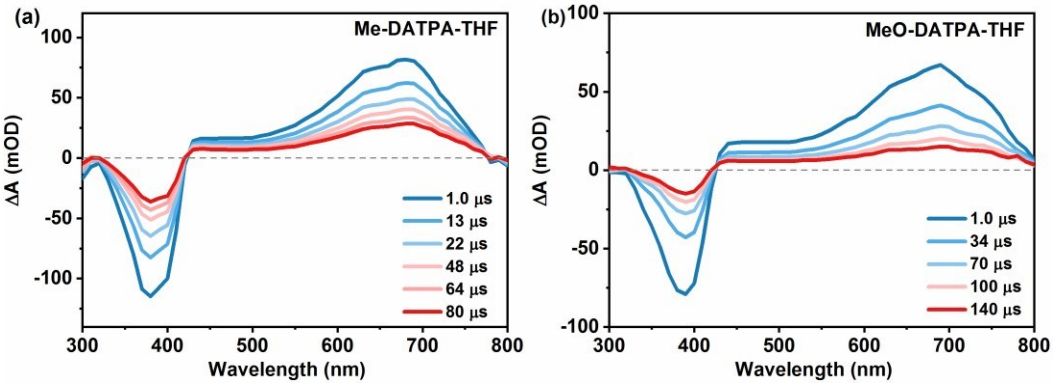

Figure S7. Nanosecond transient absorption spectra of **Me-DATPA** (a) and **MeO-DATPA** (b) in THF.

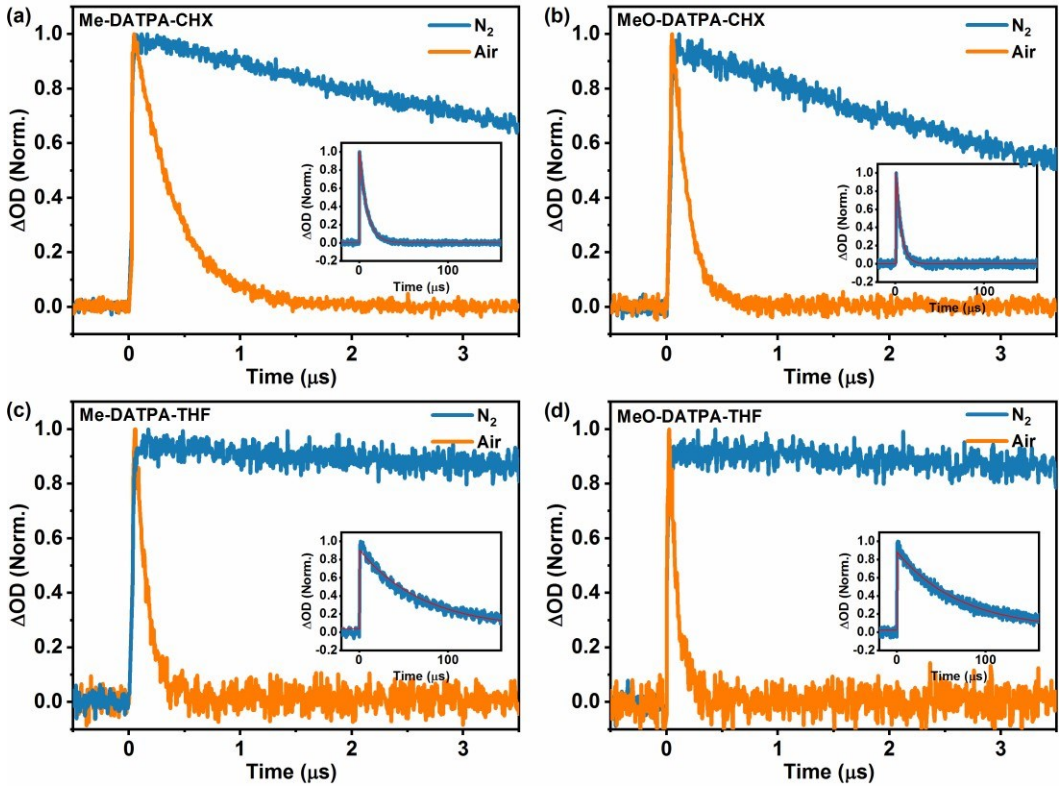

Figure S8 The kinetic traces of **Me-DATPA** and **MeO-DATPA** in CHX and THF solutions under different gas conditions (N_2, air). The lifetime of two molecules in N_2-saturated solvents is increased compared with in air-saturated solvents, indicating the long-live state is a triplet state.

References

1. Z. Kuang, G. He, H. Song, X. Wang, Z. Hu, H. Sun, Y. Wan, Q. Guo and A. Xia, *J. Phys. Chem. C*, 2018, **122**, 3727-3737.
2. M. Zhou, S. Vdovic, S. Long, M. Zhu, L. Yan, Y. Wang, Y. Niu, X. Wang, Q. Guo, R. Jin and A. Xia,
   J. Phys. Chem. A, 2013, **117**, 10294-10303.
3. Z. Kuang, H. Song, Y. Guo, Q. Guo and A. Xia, *Chin. J. Chem. Phys.*, 2019, **32**, 59-66.
4. J. S. Beckwith, A. Rosspeintner, G. Licari, M. Lunzer, B. Holzer, J. Froehlich and E. Vauthey, *J. Phys. Chem. Lett.*, 2017, **8**, 5878-5883.
5. G. Angulo, G. Grampp and A. Rosspeintner, *Spectrochimica Acta Part a-Molecular and Biomolecular Spectroscopy*, 2006, **65**, 727-731.
6. M. L. Horng, J. A. Gardecki, A. Papazyan and M. Maroncelli, *J. Phys. Chem.*, 1995, **99**, 17311- 17337.